ACS OMEGA

Open Access

http://pubs.acs.org/journal/acsodf

Article

Peptide Nucleic Acids in Saturation Transfer Difference Nuclear Magnetic Resonance Experiments: A Simple and Valuable Tool for Studying HuR–Small Molecule Complexes

Published as part of ACS Omega special issue "3D Structures in Medicinal Chemistry and Chemical Biology".

Irene Gado, Martina Garbagnoli, Francesca Alessandra Ambrosio, Roberta Listro, Michela Parafioriti, Silvia Cauteruccio, Daniela Rossi, Pasquale Linciano, Giosuè Costa, Stefano Alcaro, Francesca Vasile,* and Simona Collina*

Cite This: *ACS Omega* 2024, 9, 45147–45158

Read Online

ACCESS | Metrics & More | Article Recommendations | Supporting Information

ABSTRACT: Ribonucleic acid (RNA)-binding proteins (RBPs) play a key role in regulating RNA stability, fate, function, gene expression, post-transcriptional modifications, and cellular activities. Among the various RBPs identified to date, the Hu proteins have been the most extensively studied. Specifically, HuR influences several cellular processes, including cell proliferation, differentiation, and stress response, and it is frequently overexpressed in various solid tumors. Several HuR ligands have been identified so far, highlighting the druggability of such a protein. To discover the novel HuR–RNA interfering agents, biophysical assays represent a promising approach. To overcome limitations for RNA manipulation, in this work, we explored the use of PNA (peptide nucleic acid) as an RNA analogue in interaction studies. Molecular modeling simulation revealed the ability of aegPNA to bind HuR and, therefore, the synthesis of the designed PNA was conducted. The saturation transfer difference (STD) nuclear magnetic resonance (NMR) technique was adopted to evaluate the ability of HuR ligands to interfere with the HuR–PNA complex, comparing the obtained results with RNAs. Our results evidenced that PNA may be considered a simple and valuable tool to analyze the interaction and interfering properties of HuR ligands by STD-NMR, thus improving the precision and reliability of the approach.

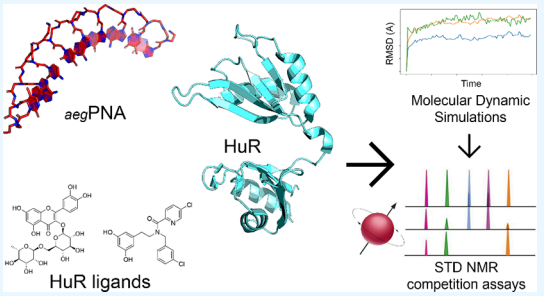

INTRODUCTION

Ribonucleic acid (RNA)-binding proteins (RBPs) recognize and interact with specific RNA sequences,[1] playing a key role in RNA stability, transport, localization, translation, and splicing, thereby regulating the fate and function of RNAs.[2,3] Among the hundreds of human RBPs, the Hu protein family (ELAV, embryonic lethal abnormal vision) has gained particular attention. HuR (ELAV1) is ubiquitously expressed and plays a central role in cell growth, proliferation, differentiation, and stress response. It is overexpressed in various solid tumors, such as glioblastoma multiforme, medulloblastoma, breast, lung, and ovarian cancers, where it is linked to tumor aggressiveness, poor prognosis, and chemotherapy resistance.[4−7] HuR also contributes to the progression of cystic fibrosis (CF). Its overexpression in CF airway epithelial cells promotes *Pseudomonas aeruginosa* adhesion by modulating Vav3. The disruption of the HuR–Vav3 mRNA complex prevents the formation of *P. aeruginosa* adhesion to the CF airway epithelium.[8]

Several studies have consistently underscored the potential of targeting HuR as a promising therapeutic strategy, confirming the importance of developing small molecules able to disrupt HuR–RNA interactions for brand-new anticancer and anti-infective targeted therapeutic interventions.[9−12]

To reach this goal, understanding the interactions between Hu proteins and mRNA is mandatory, allowing the identification of druggable binding sites for small molecules potentially able to interfere with the HuR–mRNA complex stability.[13,14]

Over the past decade, significant progress has been made in identifying and evaluating HuR ligands, including natural and synthetic compounds, for example, dehydromutacin,[15] chrysantone-like MS-444,[15] okicenone,[15] mitoxantrone,[16] diydrotanshinone-I (DHTS-I),[17] coumarins,[18] and others, thus demonstrating the druggability of this target protein.

Received: July 5, 2024
Revised: October 10, 2024
Accepted: October 16, 2024
Published: October 30, 2024

Our interdisciplinary research team has played pivotal roles in this field, employing a multifaceted approach that encompasses in silico design, virtual screening, fragment-based drug discovery, and ligand-driven NMR approaches. Through this concerted effort, we identified natural products, including epigallocatechin gallate and rutin, together with new ad hoc designed synthetic compounds, as potential HuR ligands.[13,14,19−21] Particularly, among synthetic derivatives, compounds **RBA2** and **RBA3** emerged as promising HuR ligands (Figure 1).[20]

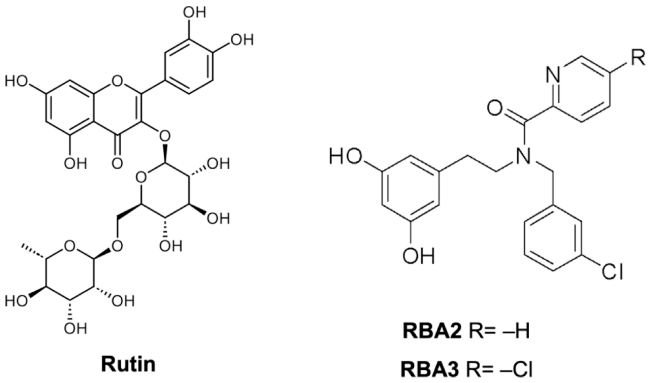

Figure 1. Structures of rutin and synthetic HuR ligands **RBA2** and **RBA3**.

However, determining whether these molecules can compete with RNA for the same or part of the binding site and thereby interfere with the formation of the HuR−RNA complex is crucial for evaluating their ability to modulate the functionality of the HuR protein and achieve the desired pharmacological effect. To this aim, biophysical techniques may be employed, as reported in a recent review on this topic.[22] Other approaches, like AlphaScreen ribonucleoimmunoprecipitation coupled with immunoblotting/RT-PCR and RNA-electrophoresis mobility shift assays (REMSAs), were typically used for low-throughput drug testing.[11,23,24] All these approaches used to evaluate the capability of HuR ligands to interfere with the HuR−RNA complex pose another challenge in this field: working with mRNA presents significant issues, since RNA is susceptible to degradation by the omnipresent ribonucleases (RNases) in the environment. Accordingly, to prevent RNA degradation, the use of certified RNase-free consumables and stringent facility hygiene standards are necessary.[25] To overcome this issue, nuclease-resistant synthetic polymers can be employed as RNA mimetics. Peptide nucleic acids (PNAs) are members of the xeno-nucleic acid family, able of mimicking both DNA and RNA.[26] The most common PNA consists of *N*-2-aminoethylglycine units (commonly known as aegPNA) decorated with typical nitrogenous bases. Unlike DNA and RNA, PNAs differ in having a peptide-like backbone instead of the typical sugar−phosphate backbone. Therefore, it is not degraded by nucleases and does not require special handling precautions.[26] Research in the field of PNAs plays a relevant role in the hot area of nucleic acid therapy as well as in the development of diagnostic, biosensor, and material sciences.[27]

In the present work, we present for the first time the development and application of a viable assay to study the ternary system of small molecule−HuR−nucleic acid, providing structural insights into the binding interactions and the ability of small molecules to impact the stability of the HuR−RNA complex. To overcome the challenges associated with RNA handling, we explored the application of aegPNA as xeno-nucleic acid for studying the HuR−ligand complexes in saturation transfer difference (STD) NMR competition assay. More in detail, through molecular modeling studies, we evaluated the ability of a selected aegPNA to recognize and bind HuR. Having the results suggested that aegPNA could be a viable alternative to RNA, we synthesized the ad hoc aegPNA fragment and investigated its ability to bind HuR and to interfere with the complexes between the three HuR ligands reported in Figure 1 and the protein. This was accomplished by performing competition STD-NMR experiments.

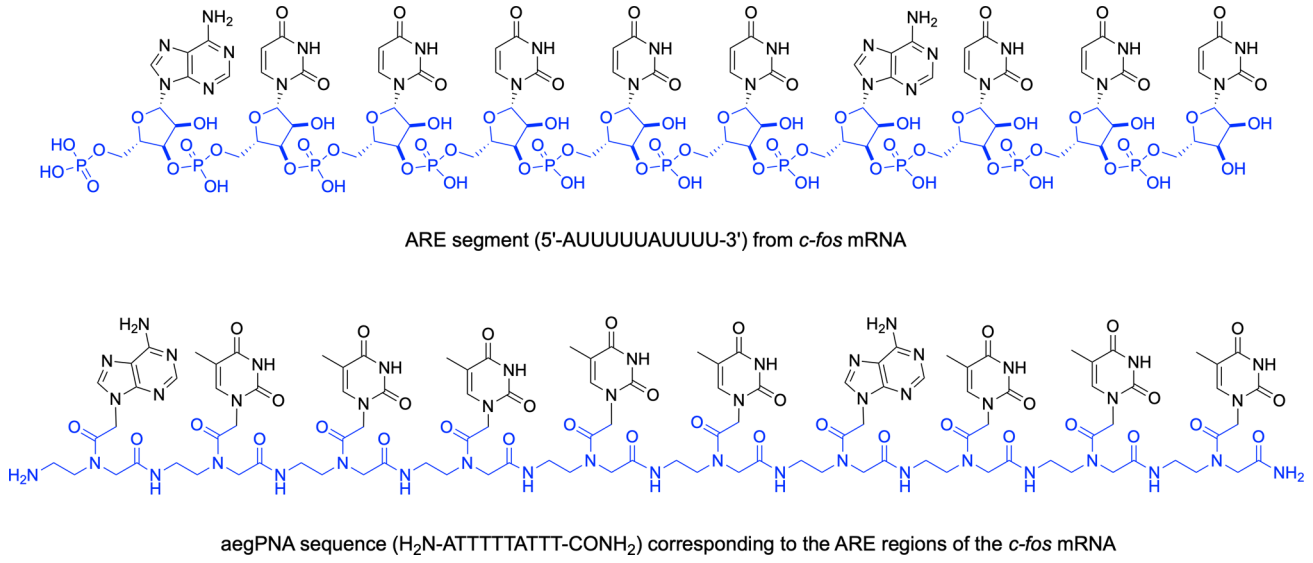

Figure 2. Alignment and comparison between the ARE segment from *c-fos* mRNA (PDB ID: 4ED5) and its corresponding designed aegPNA counterpart, H_2N-ATTTTTATTT-$CONH_2$.

https://doi.org/10.1021/acsomega.4c06244
ACS Omega 2024, 9, 45147−45158

RESULTS AND DISCUSSION

Comparison of HuR−RNA and HuR−PNA Complexes. *Exploitation of HuR−RNA Interactions for PNA Design.* Hu proteins possess three RNA-recognition motifs (RRMs) that enable them to bind with high affinity and specificity to target labile mRNAs.[28] The first two domains (RRM1 and RRM2), which are connected by a 10-residue linker, are the primary domains involved in RNA recognition and binding. They specifically interact with AU- and U-rich sequences, known as adenine−uridine-rich elements (AREs), which are typically located in the 3′-untranslated region (3′-UTR) of mRNAs. Structural studies have shown that RRM1 is the primary ARE-binding domain in HuR.[29] Upon RNA binding, a conformational change occurs that induces subsequent contacts between the interdomain linker and RRM2, enhancing the RNA-binding affinity of HuR.[30] This dynamic interaction underscores the importance of both RRMs and the interdomain linker in achieving high-affinity binding to target mRNAs. Currently, the unique crystal structure available of the HuR RRM1−2 domain complex bound to an 11-base AU-rich segment (5′-AUUUUUAUUUU-3′) from *c-fos* mRNA (PDB ID: 4ED5) provides a detailed view of the binding interface and specific molecular interactions.[30] This structure reveals an intricate network of contacts between the HuR RRMs and the AU-rich RNA sequence, highlighting the critical residues involved in RNA recognition and binding. Based on the structural insights gained from the HuR−RNA complex, we designed a PNA decamer corresponding to the AU-rich regions of the *c-fos* mRNA, crucial for HuR binding. We selected a backbone derived from *N*-2-aminoethylglycine PNA (aegPNA) and replaced the uracil of *c-fos* mRNA with thymine, since it has been demonstrated that it shows the same general behavior observed for uracil, due to rather similar electronic structures.[31] Moreover, the higher chemical stability of thymine makes it easier to handle for synthetic purposes and the methyl in C5 on thymine confers higher stability than uracil, especially in a biological environment.[32,33]

Based on the above considerations, we selected the aegPNA sequence (H_2N-ATTTTTATTT-CONH$_2$), which is reported in Figure 2 in comparison with *c-fos* mRNA as a substitute of mRNA to perform HuR−small molecule (SMol) competitive studies.

Molecular Docking and Molecular Dynamic Studies. To validate the PNA design, we performed molecular docking and molecular dynamic simulations. Docking results revealed that aegPNA can bind the same region of HuR occupied by the RNA (Figure 3) with a good theoretical binding affinity (−223.23 kcal/mol). Furthermore, the docking analysis of the aegPNA binding mode showed that it formed a hydrogen bond with Tyr63 and several hydrophobic contacts with the amino acid residues lying in the cavity.

A set of three replicate simulations of 200 ns were carried out for HuR-mRNA and HuR-aegPNA complexes, highlighting that in the presence of the aegPNA after a period of rearrangement, the protein undergoes toward a conformational transition to a new stable state, which better accommodates the aegPNA (Figure 4).

Moreover, the RMSD trend of the aegPNA was calculated in order to evaluate how stable it is concerning the protein and its binding site, and noteworthy, a good stability of the aegPNA in the HuR binding site was found throughout the whole simulation, mimicking the behavior of the mRNA strand (Figure 5).

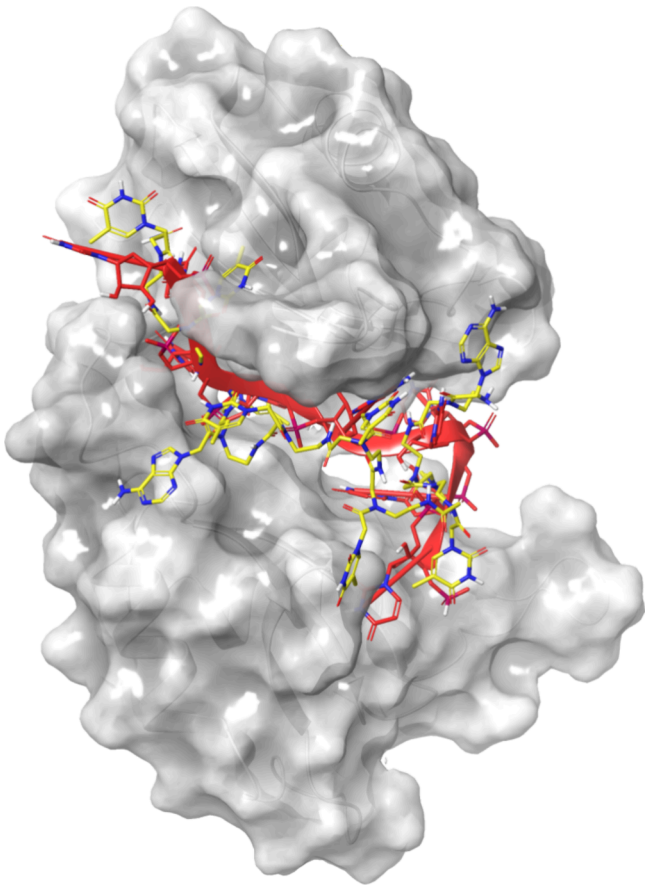

Figure 3. 3D representation of HuR in complex with the best docking poses of mRNA and the aegPNA, obtained with the HDOCK tool. The protein is shown as a gray surface, the mRNA is shown as a red cartoon, while meanwhile, the aegPNA is shown as yellow carbon sticks. Atomic coordinates were obtained from the PDB model 4ED5.

Finally, for each replica, the protein interactions with the PNA were monitored throughout the simulation, and as reported in Figure 6 and Figure SI-6, we found that PNA is able to maintain several long-lasting interactions with the key residues of the HuR binding site.

Significantly, by analyzing the histogram, we found that most of the long-lasting interactions established between the aegPNA and HuR key residues, such as Tyr63, Arg97, Tyr109, Arg153, Arg136, and Asn25, are likewise observed in the HuR−mRNA complex (Figure SI-7).

To summarize, our modeling analysis suggested that the aegPNA binds the protein in the same site recognized by the *c-fos* RNA and highlighted that aegPNA stabilizes HuR and its binding site.

PNA Synthesis. Prompted by computational HuR−RNA/PNA interaction studies, we synthesized the aegPNA sequence for STD-NMR experiments. Specifically, the fragment H_2N-ATTTTTATTT-CONH$_2$ was prepared manually through the solid-phase synthesis using the Boc/Z strategy, according to the well-established protocols reported in the literature (Scheme 1).[34] Starting from the commercially available MBHA resin, the synthesis of aegPNA began with the downloading of the resin with the first PNA monomer (loading 0.2 mmol/g), followed by the iterative addition of the

https://doi.org/10.1021/acsomega.4c06244
ACS Omega 2024, 9, 45147−45158

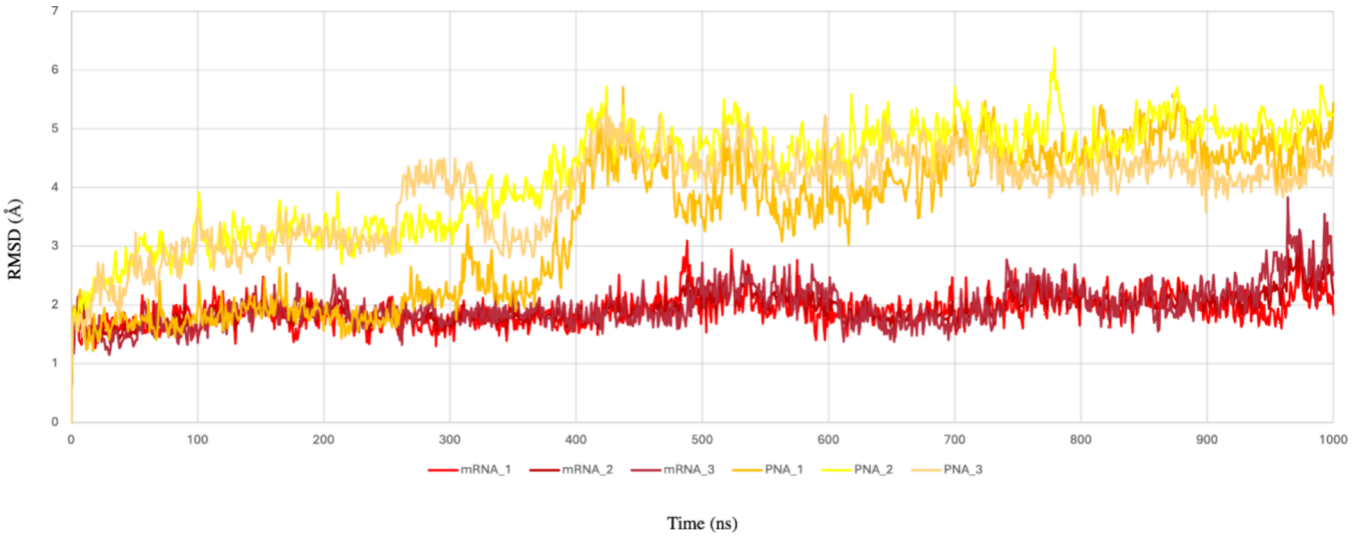

Figure 4. HuR protein backbone RMSD trend, obtained from three replica performed for each system and calculated in the presence of aegPNA (dark-yellow, salmon, and yellow lines) and RNA (red, brown, and dark-red lines). The RMSD values are expressed in Å.

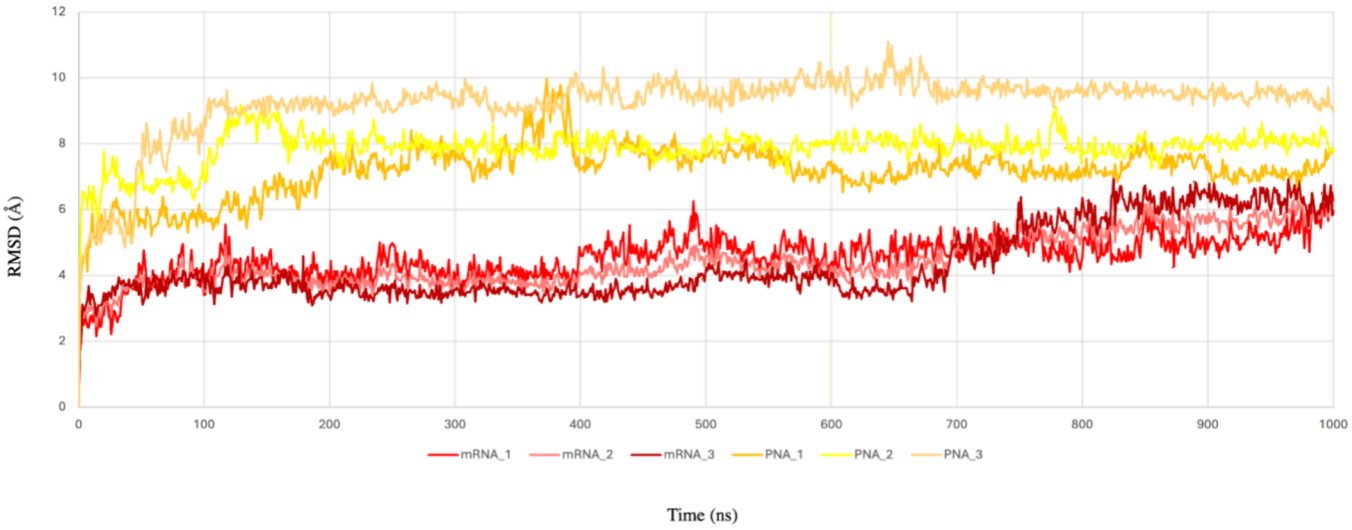

Figure 5. RMSD plot, obtained from three replica performed for each system, of aegPNA (dark-yellow, salmon, and yellow lines) and RNA (red, brown, and dark-red lines). The RMSD values are expressed in Å.

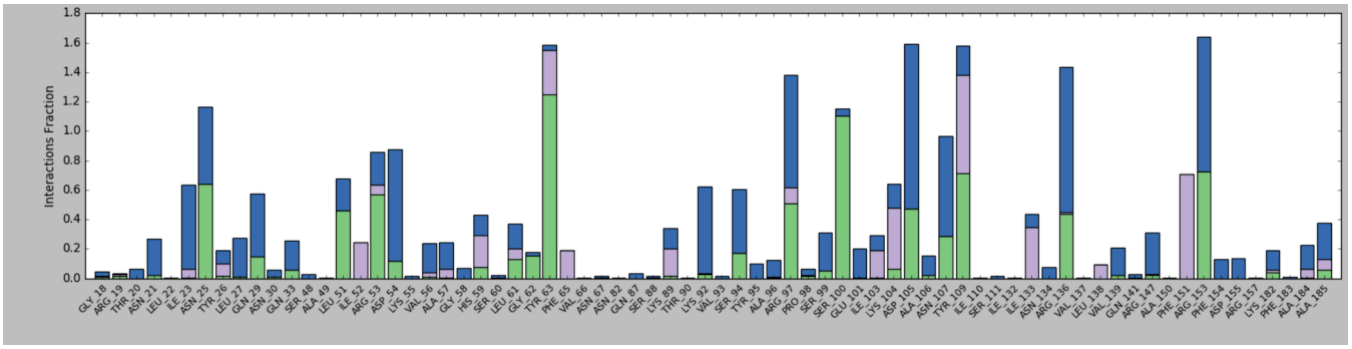

Figure 6. Histogram of protein−ligand interactions monitored throughout the whole simulation. The residues' numbers involved in the interactions with the aegPNA are reported on the *x*-axis, and the fraction of interactions is reported on the *y*-axis. The hydrogen bonds, the hydrophobic contacts, and the water bridges interactions are reported in green, violet, and blue, respectively.

remaining nine monomers. Each cycle consisted of three steps: (i) deprotection of the Boc group from the amino group of the aminoethylglycine backbone of the monomer attached to the resin under acidic conditions using a mixture of TFA/*m*-cresol; (ii) coupling between the free amino group of the monomer on the resin and the −COOH group of the next monomer in the sequence, using HATU as a condensing agent and DIPEA as a base in NMP as a solvent; (iii) capping of the unreacted

https://doi.org/10.1021/acsomega.4c06244
ACS Omega 2024, 9, 45147−45158

Scheme 1. General Procedure for the Synthesis of aegPNA Decamer

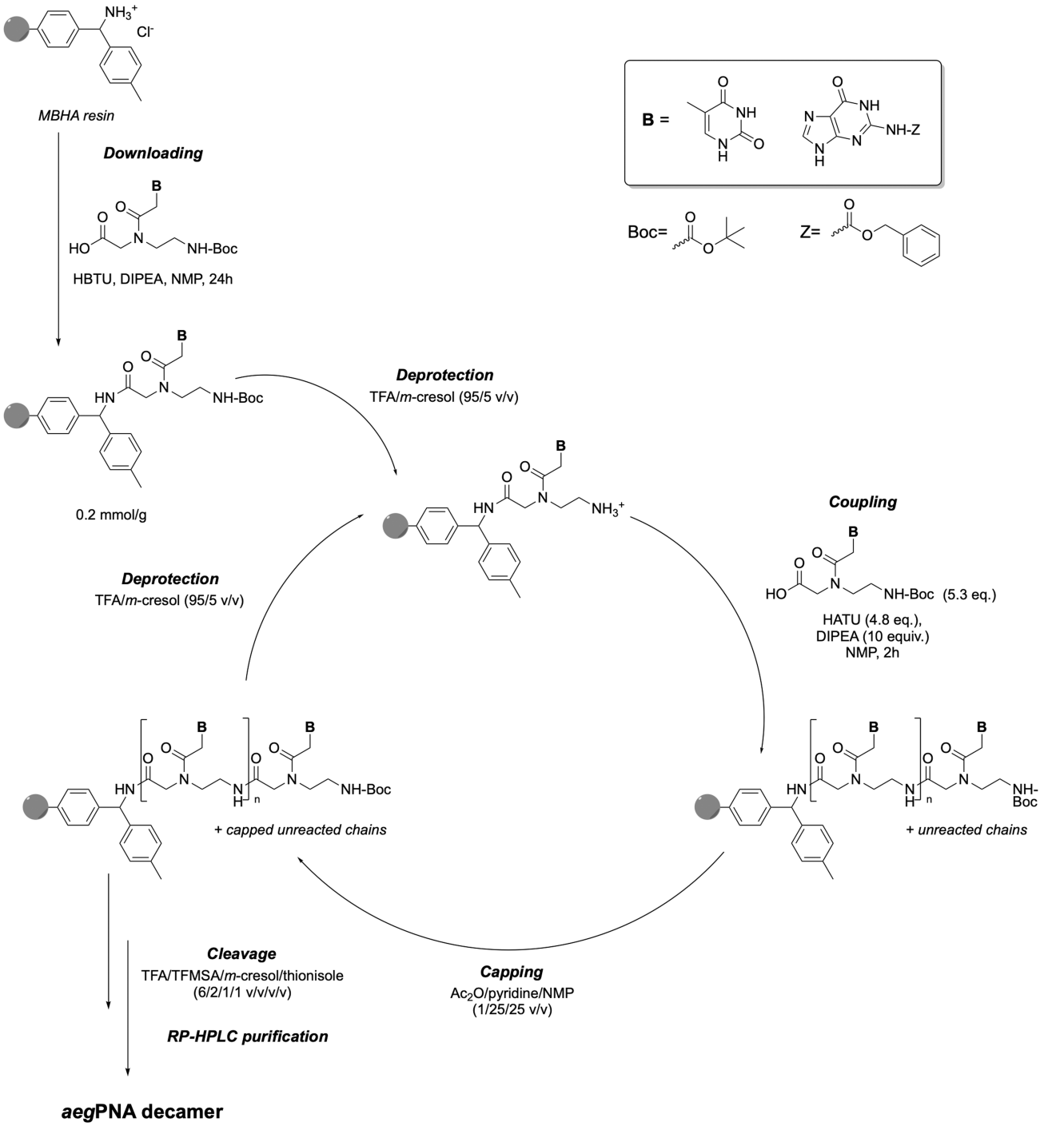

chains using a mixture of acetic anhydride, pyridine, and NMP. Lastly, the resin-supported aegPNA decamer was subjected to cleavage under acidic conditions, using a mixture of TFA/TFMSA/*m*-cresol/thioanisole (Scheme 1). The crude aegPNA was then purified by means of RP-HPLC, using a semi-preparative column. The purified aegPNA was analyzed by UPLC-HR-ESI$^+$ mass analysis (see the Supporting Information) that confirmed its identity and purity (Figure SI-1).

STD-NMR Studies. The STD-NMR experiment is a fast and powerful technique for detecting transient binding of small molecules (present in excess) to a protein, making it useful for screening and assessing binding interactions. In STD-NMR, the macromolecule is selectively irradiated at a frequency that excites only its protons, transferring magnetization to the bound ligands. This leads to changes in the signal intensity of protons due to the nuclear Overhauser effect (nOe), providing insights into binding interactions. The data processing produces a one-dimensional spectrum that displays only the signals from protons interacting with the protein, resulting in a spectrum of the epitope.

First, we studied the interaction between the protein and the selected RNA fragment. The spectrum (Figure SI-2) showed that a strong interaction occurs between the protein and the nucleic acid, even if it does not provide specific details on how

https://doi.org/10.1021/acsomega.4c06244
ACS Omega 2024, 9, 45147−45158

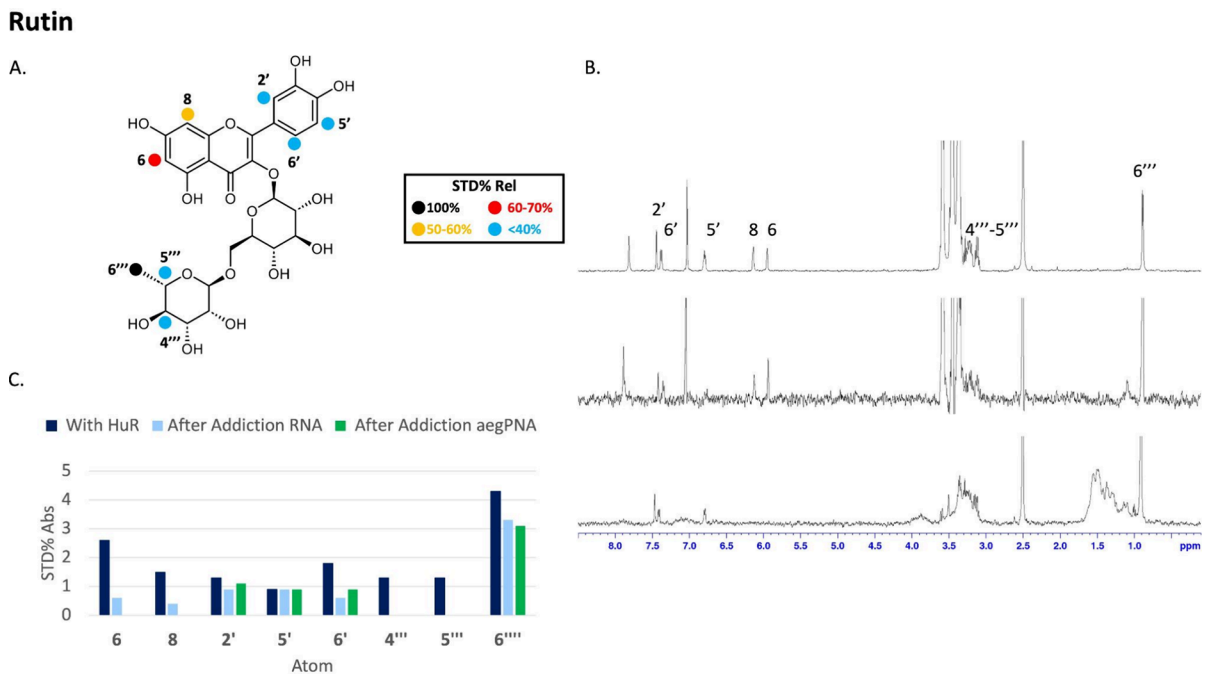

Figure 7. (A) Epitope map of rutin with relative STD percentages conveyed by color code. Legend indicates in black the most intense signal (100% relative STD), in red the relative STD over 60%, in yellow the relative STD over 50%, and in light blue the relative STD under 40% in relationship to the most intense STD signal. (B) From above to below: ^{1}H NMR of rutin in the presence of HuR in PBS pH 7.4; STD spectrum of rutin in the presence of HuR; STD spectrum of rutin in the presence of HuR and aegPNA. (C) STD intensities (%) of rutin in the presence of HuR (blue) and after the addition of RNA (light blue) and aegPNA (green).

the nucleobases are involved in the interaction. STD-NMR offers important insight into the RNA−protein interactions, providing a tool for identifying binding determinants. The comparison between the reference and STD spectra suggested a strong interaction for the aromatic protons of the nucleobases but also an intense engagement of the ribose protons (as evidenced by the presence of the peaks around 5.5 ppm and in the range between 3.5 and 4.3 ppm). This data confirmed that the entire RNA sequence is well arranged in the protein binding pocket with the involvement of all nucleotides, indicating an agreement with crystal and computational structures.[30]

The binding interaction of the synthesized aegPNA with HuR was confirmed by NMR experiments. The 1D ^{1}H NMR spectrum of the aegPNA fragment reveals the presence of broad peaks due to exchange processes on the NMR time scale. This effect can be caused by the nuclear spin experiencing more than one magnetic environment as a result of conformational changes in the molecule (such as slow rotation around the C−N amide bonds). The different residues of the sequence cannot be distinguished, but the chemical moieties of aegPNA residues can be identified: in the range 8−8.5 ppm, the chemical shift of the adenine purine ring can be observed while around 7.3 ppm, and the chemical shift of pyrimidine protons is visible. Also, the protons of the peptidic backbone and of the methyl groups of thymine are assignable. In the STD-NMR experiment (Figure SI-3), the STD difference spectrum features the peaks of all of the moiety, implying that all of the protons are involved in the binding with the protein. In the STD experiment (Figure SI-3), all the moieties are visible and all the protons are involved in the epitope, confirming a good binding with the protein. In particular, a good interaction is observed not only for the aromatic protons of the bases but also for methyl groups and the methylene protons of the backbone. Overall, we proved the ability of aegPNA to bind HuR such as the RNA fragment.

STD-NMR Competition Studies for the Analysis of the Interaction of HuR Ligands in the Presence of PNA. Encouraged by these results, to challenge the idea of PNA as an RNA mimetics, we exploited STD-NMR to study the aegPNA potential during STD-NMR competition studies with three reference small molecules (Figure 1) already identified as HuR−RNA complex interferents. A first set of experiments was performed using rutin, selected as model compound since it has been already studied by combining molecular modeling and STD-NMR experiments.[13,21]

To confirm that the binding of rutin to HuR occurs in the RNA binding site, we performed further STD-NMR studies by adding the AU-rich fragment as a competitor to the HuR−rutin complex. STD values for rutin protons were calculated both in the absence and upon addition of RNA (Figures SI-4 and SI-5) showing that rutin STD intensities strongly decreased. In particular, the aromatic protons of the flavonoid nucleus are strongly reduced, and some protons of the sugar ring disappear. The signals of RNA appear in the STD spectrum, confirming its high affinity for the protein and showing that it can displace rutin from the binding site. This data confirm that the binding of rutin to HuR occurs in the RNA binding site.

Hence, to confirm aegPNA as a mimic of RNA, we performed STD-NMR experiments adding PNA as a competitor to the rutin−HuR complex. A reduction of rutin STD absolute values after the addition of PNA was evidenced both for the chromone-3-ol and aromatic moieties and for the sugars, similar to what was observed in the presence of RNA, also confirming the same binding site for rutin and the nucleic acids. The experimental results are in agreement with those predicted, confirming that PNA behaves as RNA. Specifically,

https://doi.org/10.1021/acsomega.4c06244
ACS Omega 2024, 9, 45147−45158

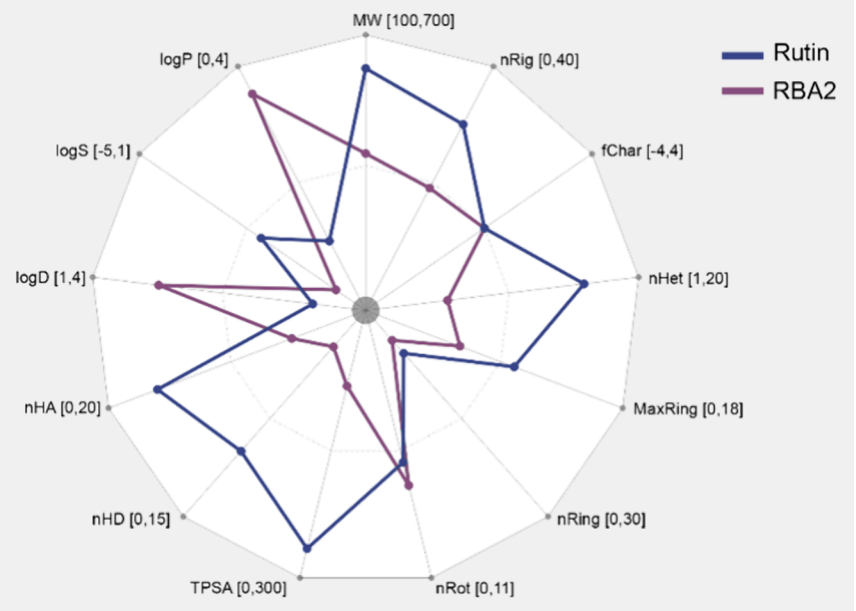

Figure 8. Physicochemical properties of rutin and **RBA2**. The computed physicochemical parameter abbreviations and the upper and lower limits for druggability are reported in the Experimental Section. The range of the axis for each parameter is reported in squared bracket. Figure adapted from ADMETLab 2.0.

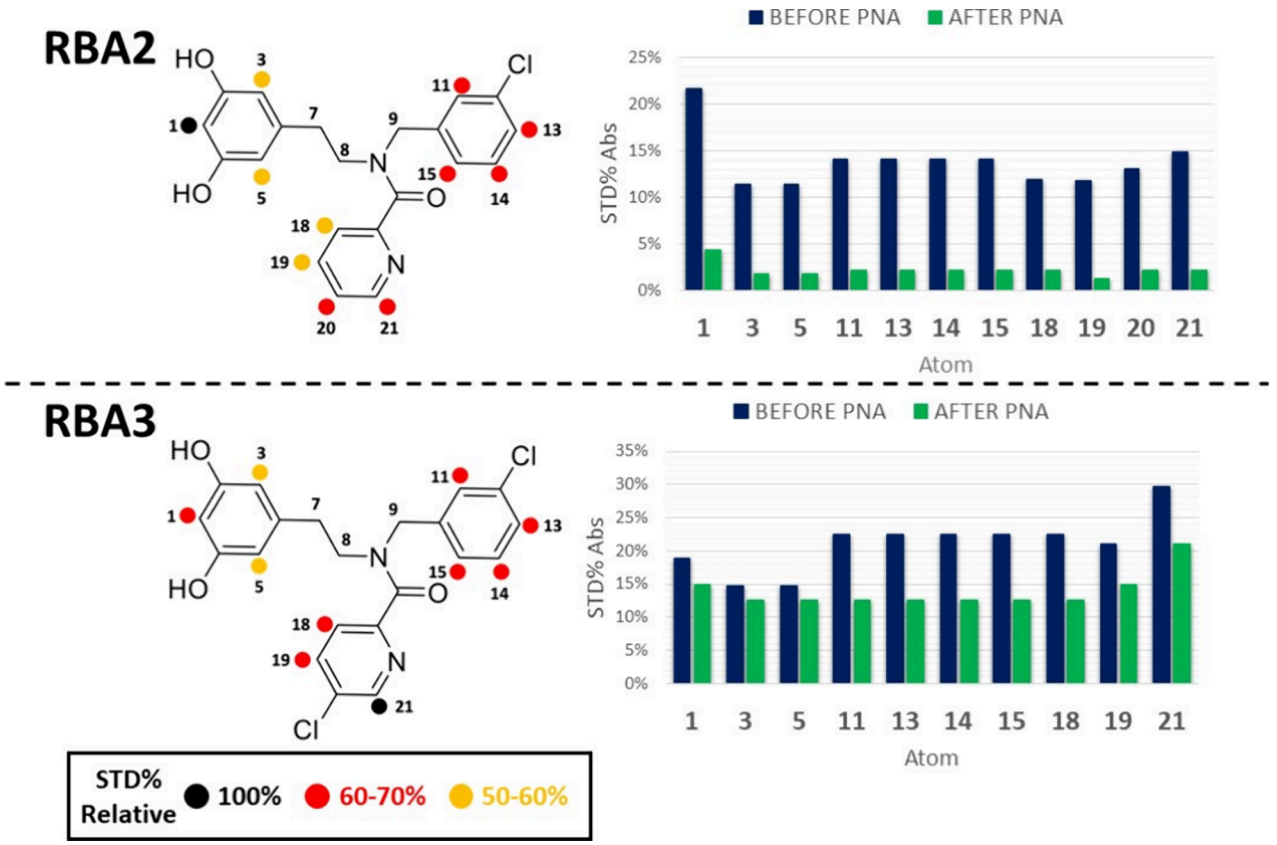

Figure 9. Epitope map of compound **RBA2** and **RBA3** with relative STD percentages conveyed by color code. Legend indicates in black and red the relative STD over 60%, in yellow over 50%, and in light blue under 40%; all relative to the most intense STD signal. STD intensities (%) of **RBA2** and **RBA3** are reported in histograms before (blue) and after (green) the addition of aegPNA fragment. **RBA2** and **RBA3** spectra and tables are reported in the Supporting Information (Figures SI-9 and SI-10).

some protons of the flavonoid moiety and of sugar disappear while others show a decrease in their STD intensity (Figure 7). The presence in the STD spectrum of strong aegPNA signals confirms its strong interaction with HuR and shows the ability of aegPNA to displace rutin from its binding site as already observed for RNA.

https://doi.org/10.1021/acsomega.4c06244
ACS Omega 2024, 9, 45147−45158

To validate the suitability of competition assay in the presence of aegPNA, we extended the analysis to **RBA2** and **RBA3**.[19] The direct binding of these two synthetic compounds with HuR was already demonstrated by STD-NMR, and the ligand binding epitopes were highlighted. The binding mode was postulated through molecular modeling suggesting the binding of the two small molecules within the mRNA−binding cleft, occupying more in detail the subpocket involved in the interaction with U8 and U9 of the transcript.[20] This was further supported by fluorescence polarization (FP) studies highlighting their potential to interfere with the formation of the HuR−mRNA complex.[20] Rutin, **RBA2**, and **RBA3** are different in terms of molecular space and structural properties as shown by the graphics representing their physicochemical properties (Figure 8). As examples, rutin is endowed with a higher molecular weight (more than 600 g/mol), a flexibility of 0.200, and a log *P* of −0.038. **RBA** derivatives are smaller (molecular weight of around 400g/mol), more flexible (around 0.300), and more lipophilic (log *P* around 4.00). Moreover, the compounds show differences even in terms of number of hydrogen-bond donor (nHD) and acceptor (nHA): nDH and nHA of rutin are, respectively, 5-fold and 2-fold higher than the **RBA** ones.

In STD-NMR competition assays, **RBA2** and **RBA3** binding epitopes were determined in the presence of aegPNA. The addiction of aegPNA to the ligand−HuR complexes causes a strong decrease in the intensity of all compound signals, indicating that both aegPNA and **RBA** compounds can bind the same binding pocket on the target protein. In the case of **RBA2**, an estimated decrease of 5 to 7 times for all visible protons in terms of absolute STD % was shown (Figure 9). In the case of **RBA3** (Figure 9), a limited reduction in STD intensities was observed, suggesting a stronger **RBA3**−protein interaction compared to those of **RBA2** and rutin. Specifically, the **RBA3** STD peaks upon the addition of aegPNA decrease to approximately half their original intensity. The quantitative analysis of the STD value reduction for **RBA2** and **RBA3** after the addition of aegPNA allowed us to hypothesize that **RBA3** has a high affinity for HuR.

Thus, after the aegPNA addition, the reduction of the **RBA2** and **RBA3** signals is accompanied by the presence in the STD spectrum of the signals of the protons belonging to the aegPNA. These data suggest that both aegPNA and **RBA** compounds are competing with the same binding site on the target protein, thus highlighting their ability to interact with the same binding site of RNA.

CONCLUSIONS

The present study adds a piece to the puzzle of our medicinal chemistry efforts in finding effective small molecules that can disrupt the HuR−RNA interaction, a promising target in cancer therapy. The need to understand the ternary system small molecule−HuR−nucleic acid is critical, and there is a need to develop rapid and viable processes, useful to provide at the same time structural insights important for drug design as well as the stability of the complexes. Current techniques for evaluating the binding of putative ligands with RBP and, in particular, with HuR mainly rely on SPR or STD-NMR. The former allows real-time data on binding kinetics and affinities, offering a quantitative understanding of the interaction, whereas the latter is useful for obtaining structural insight into the ligand epitope. Thus, these methods can be exploited at the beginning of the pipeline to identify and assess the binding capability of small molecules for HuR. However, few methods are capable of both confirming that a ligand binds directly to the RNA-binding site and assessing its potential to displace RNA, each with its own limitations. To this aim, we selected STD-NMR as the most suitable technique. Since the instability of RNA poses significant challenges in STD-NMR, due to its susceptibility to environmental degradation, we employed both molecular modeling and STD-NMR to demonstrate that aegPNA can effectively mimic the RNA role in binding to HuR. Our modeling analysis showed that aegPNA effectively has the ability to bind the same binding site on HuR as the *c-fos* RNA. Subsequent STD-NMR experiments confirmed these interactions and demonstrated that aegPNA could be effectively used in competition assays displacing small molecules. The reduction in STD signals with aegPNA, comparable to those observed with RNA, validated PNA's utility for studying HuR−ligand interactions.

To sum up, aegPNA represents a robust alternative to RNA in a competition STD-NMR assay. This pioneering approach not only overcomes the challenges of RNA degradation but also lays the groundwork for optimizing screening methods for potential agents that interfere with the HuR−RNA complex, potentially expediting the identification of novel therapeutic agents targeting this pathway and offering a beneficial alternative for advancing studies on RBP−ligand interactions. Ultimately, this strategy enhances drug discovery efforts targeting HuR and opens new avenues for therapeutic interventions against cancer.

EXPERIMENTAL SECTION

STD-NMR. All protein−ligand samples were prepared in a 400:1 ligand:protein ratio, while the samples with aegPNA had a ligand:PNA:protein ratio of 400:200:1. The final concentration were 2 mM of ligand, 1 mM of aegPNA decamer, and 5 μM of HuR. The final volume in a 3 mm NMR tube was 180 μL. The buffer used was a 20 mM deuterated phosphate buffer at pH 7.4. A percentage (less than 10%) of DMSO-d_6 was added when necessary to improve the solubility of the small molecules. ^{1}H-STD-NMR experiments were performed on a 600 MHz Bruker Avance spectrometer. The probe temperature was maintained at 298 K. In the STD experiments, water suppression was achieved by the excitation-sculpting pulse sequence (*stddiffesgp*). The on-resonance irradiation of the protein was performed at −0.05 ppm. Off-resonance irradiation was applied at 40 ppm, where no protein signals were visible. Selective presaturation of the protein was achieved by a train of Gauss-shaped pulses of 50 ms length each. The STD-NMR spectra were acquired with an optimized saturation time of 2 s. Blank experiments were conducted in the absence of protein in order to avoid artifacts or false positives. STD spectra in the absence of the ligands did not show relevant signals. The different signal intensities of the individual protons are best analyzed from the integral values in the reference and STD spectra, respectively. $(I_0 - I_{sat})/I_0$ is the fractional STD effect, expressing the signal intensity in the STD spectrum as a fraction of the intensity of an unsaturated reference spectrum. In this equation, I_0 is the intensity of one signal in the off-resonance or reference NMR spectrum, I_{sat} is the intensity of a signal in the on-resonance NMR spectrum, and $I_0 - I_{sat}$ represents the intensity of the STD-NMR spectrum. For NMR studies, HuR was obtained as previously reported,[17] **RBA2** and **RBA3** were synthesized and purified as reported in the already published article,[20] the rutin and AU-

https://doi.org/10.1021/acsomega.4c06244
ACS Omega 2024, 9, 45147−45158

rich fragment of the *c-fos* 3′ UTR mRNA (5′-AUUUUUAUUUU-3′) was bought by Sigma-Aldrich Corporation, and aegPNA was obtained as described in the following paragraph.

Synthesis of aegPNA. aegPNA was synthesized by solid-phase synthesis using Boc/Z chemistry.[34] The monomers Boc-PNA-T−OH (>95%) and Boc-PNA-A(Z)−OH (>95%) were purchased from ASM Research Chemicals GmbH (Hannover, Germany). The polystyrene MBHA resin (0.88 mmol/g) was purchased from Novabiochem. Polypropylene one-way syringes and the corresponding polytetrafluoroethylene (PTFE) frits, used as a reactor for the manual solid-phase synthesis, were purchased from Alltech Associates Inc. (Lokeren, Belgium). The reverse-phase RP-HPLC purification was performed on an Agilent 1200 Series system, using the semipreparative Luna C18 column (25 cm × 10 nm, 5 μm). A binary mixture of solvents A (water + 0.1% TFA) and B (acetonitrile + 0.1% TFA) was used as a mobile phase. UPLC-MS analyses were performed on an Acquity UPLC I-class instrument (Waters, Milford, MA, USA) equipped with an Acquity UPLC PDA detector (Waters) and interfaced with a Synapt G2-S*i* QToF high-resolution mass spectrometer (Waters) through a Zspray ESI-probe for electrospray ionization (Waters). Chromatographic separations were achieved on an ACQUITY UPLC BEH C18 (100 × 2.1 mm, 1.7 μm) column (Waters) fitted with a VanGuard cartridge (Waters) and kept at 35 °C. Eluents were: water + 0.1% formic acid (solvent A) and acetonitrile + 0.1% formic acid (solvent B). A linear elution gradient was applied (5 to 45% of solvent B in 5 min) at a constant flow rate of 0.4 mL/min, followed by a column wash and re-equilibration (run-to-run time 11 min). The absorbance of the LC eluate was recorded at 260 nm. High-resolution mass spectra were acquired over the m/z range 500−1500 in a positive polarity (HR-ESI$^+$ MS). Data were processed with a MassLynx v4.2 software (Waters), and the deconvoluted HR-MS spectra were obtained using an integrated MaxEnt tool.[35]

HR-ESI$^+$ MS: m/z found (calculated): 1349.0392 (1349.0396) $[M+2H]^{2+}$, 899.6935 (899.6955) $[M+3H]^{3+}$, 684.5088 (684.5124) $[M+3H+K]^{4+}$. From the deconvolution of the signal: found 2697.0706 (calc. for $C_{110}H_{142}N_{47}O_{36}$, 2697.0726) $[M + H]^+$. The HR-ESI mass spectrum also displays signals related to multicharged adducts with sodium and potassium.

Molecular Modeling Studies. The crystallographic structure of the two N-terminal RRM domains of HuR in complex with the ARE sequence of *c-fos* RNA (PDB ID: 4ED5) was used for computational studies.[30] The structure was properly processed using the Protein Preparation Wizard tool.[36] Hydrogens were added, and disulfide bonds were created. Missing side chains and missing loops were added by using Prime. The hydrogen bonding network was optimized, and the pK_a values of the residues along with their protonation state were calculated at pH 7.4. The structure was then submitted to energy minimization steps, using OPLS_2005 as a force field.[37] The aegPNA was prepared and optimized by means of Protein Preparation Wizard tool[37] using OPLS_2005 as a force field and pH 7.4. The docking simulations were performed using the HDOCK server,[38] which is based on a hybrid algorithm of template-based modeling and ab initio free docking useful to predict the binding affinity between proteins and protein−DNA/RNA complexes. The PDB structures were uploaded into the HDOCK server as receptor and ligand, using default settings.

In detail, for the docking of mRNA, we uploaded as an input receptor molecule the PDB file of HuR protein (PDB ID: 4ED5) and as an input ligand molecule the mRNA sequence saved as PDB file. For the aegPNA docking, we uploaded as input receptor molecule the PDB file of HuR protein (PDB ID:4ED5) and as an input ligand molecule the aegPNA sequence saved as PDB file.

Docking results reveal that mRNA binds HuR with a good theoretical binding affinity (−696.46 kcal/mol). The best docking solution presents a Root Mean Square Deviation (RMSD) value equal to 3.4 Å with respect to the experimentally determined binding mode (Figure SI-8), thus validating our docking approach.

After the docking calculations, the result files with the docking scores and docked structures were retrieved from the server. The docked structures, in PDB format, were directly loaded on Schrödinger 2018-1[39] for structure inspection and for the following computational studies.

To evaluate the stability of HuR in the presence of the aegPNA and mRNA, a set of three replicate simulations of 200 ns of molecular dynamic simulations (MDs) were carried out. The MDs were run using Desmond package v5.3 at 300 K temperature and ensemble NPT class.[40] The system was immersed in an orthorhombic box of TIP4P water molecules, extending at least 10 Å from the protein, and counterions were added to neutralize the system charge. Subsequently, for each system, the simulation interaction diagram tool implemented in Desmond v5.3 was used to analyze the trajectory.[41] The analysis included protein and ligand RMSD and protein ligand contacts calculations evaluated during the whole simulation.

Physicochemical properties of the ligand's evaluations were carried out using the ADMETlab 2.0 software. The following parameters/properties have been considered: MW (molecular weight, optimal: 100−600, based on the drug-like soft rule), nRig (number of rigid bonds, optimal: 0−30, based on the drug-like soft rule), fChar (formal charge, optimal: −4 to 4, based on the drug-like soft rule), nHet (number of heteroatoms, optimal: 1−15, based on the drug-like soft rule), MaxRing (number of atoms in the largest ring, optimal: 0−18, based on the drug-like soft rule), nRing (number of ring systems, optimal: 0−30, based on the drug-like soft rule), nRot (number of rotatable bonds, optimal: 0−11, based on the drug-like soft rule), TPSA (total polar surface area, 0−140, based on the Veber rule), nHD (number of hydrogen-bond donors, optimal: 0−7, based on the drug-like soft rule), nHA (number of hydrogen-bond acceptors, optimal: 0−12, based on the drug-like soft rule), Log *D* (logarithm of the *n*-octanol/water distribution coefficient at pH 7.4, optimal: 1−3 log mol/L), Log *S* (logarithm of aqueous solubility, optimal: −4 to 0.5 log mol/L), Log *P* (logarithm of the *n*-octanol/water distribution coefficient, optimal: 0−3 log mol/L). Figure generated using ADMETLab 2.0.[42,43]

■ ASSOCIATED CONTENT

Supporting Information

The Supporting Information is available free of charge at https://pubs.acs.org/doi/10.1021/acsomega.4c06244.

Figure SI-1: UPLC-PAD trace (λ = 260 nm) for aegPNA and HR ESI-MS spectrum of the corresponding peak at 3.30 min; Figure SI-2: (A) ^{1}H NMR of RNA in the

https://doi.org/10.1021/acsomega.4c06244
ACS Omega 2024, 9, 45147−45158

presence of HuR in PBS pH 7.4; (B) STD spectrum of RNA in the presence of HuR; Figure SI-3: (A) ^{1}H NMR of PNA in the presence of HuR in PBS pH 7.4; (B) STD spectrum of PNA in the presence of HuR.; Figure SI-4: (A) ^{1}H NMR of rutin in the presence of HuR in PBS pH 7.4; (B) STD spectrum of rutin in the presence of HuR; Figure SI-5: (A) ^{1}H NMR of rutin in the presence of HuR and RNA in PBS pH 7.4; (B) STD spectrum of rutin in the presence of HuR and RNA; Figure SI-6: Histogram of protein−ligand interactions monitored throughout the whole simulation; the residues' numbers involved in the interactions with the aegPNA are reported on the *x*-axis, and the fraction of interactions is reported on the *y*-axis; the hydrogen bonds, the hydrophobic contacts, and the water bridges interactions are reported in green, violet, and blue, respectively; Figure SI-7: Histogram of protein−ligand interactions monitored throughout the whole simulation, for each replica; the residues' numbers involved in the interactions with the mRNA are reported on the *x*-axis, and the fraction of interactions is reported on the *y*-axis; the hydrogen bonds, the hydrophobic contacts, ionic, and the water bridges interactions are reported in green, violet, magenta, and blue, respectively; Figure SI-8: 3D representation of mRNA experimentally determined binding mode (green sticks) and mRNA best docking pose (red sticks) obtained by using the HDOCK tool; Figure SI-9: (A) 1H-NMR of RBA2 in the presence of HuR in PBS pH 7.4; (B) STD spectrum of **RBA2** in the presence of HuR; (C) STD spectrum of **RBA2** in the presence of HuR and aegPNA; Table SI-1: STD intensities (%) of **RBA2** before and after the addition of PNA; Figure SI-10: (A) ^{1}H NMR of **RBA3** in the presence of HuR in PBS pH 7.4; (B) STD spectrum of **RBA3** in the presence of HuR; (C) STD spectrum of **RBA3** in the presence of HuR and aegPNA; Table SI-2: STD intensities (%) of **RBA3** before and after the addition of PNA (PDF)

Accession Codes

[#]I.G. and M.G contributed equally.

AUTHOR INFORMATION

Corresponding Authors

Francesca Vasile − *Department of Chemistry, University of Milan, Milano 20133, Italy*; Email: francesca.vasile@unimi.it

Simona Collina − *Department of Drug Sciences, University of Pavia, Pavia 27100, Italy*; orcid.org/0000-0002-2954-7558; Email: simona.collina@unipv.it

Authors

Irene Gado − *Department of Chemistry, University of Milan, Milano 20133, Italy*

Martina Garbagnoli − *Department of Drug Sciences, University of Pavia, Pavia 27100, Italy*

Francesca Alessandra Ambrosio − *Dipartimento di Scienze della Salute, Università "Magna Græcia" di Catanzaro, Catanzaro 88100, Italy*; orcid.org/0000-0003-4874-2946

Roberta Listro − *Department of Drug Sciences, University of Pavia, Pavia 27100, Italy*; orcid.org/0000-0001-7615-1284

Michela Parafioriti − *Department of Chemistry, University of Milan, Milano 20133, Italy; Department of Drug Sciences, University of Pavia, Pavia 27100, Italy*

Silvia Cauteruccio − *Department of Chemistry, University of Milan, Milano 20133, Italy*; orcid.org/0000-0002-9540-9073

Daniela Rossi − *Department of Drug Sciences, University of Pavia, Pavia 27100, Italy*

Pasquale Linciano − *Department of Drug Sciences, University of Pavia, Pavia 27100, Italy*; orcid.org/0000-0003-0382-7479

Giosuè Costa − *Dipartimento di Scienze della Salute, Università "Magna Græcia" di Catanzaro, Catanzaro 88100, Italy; Net4Science Academic Spin-Off, Università "Magna Græcia" di Catanzaro, Catanzaro 88100, Italy*; orcid.org/0000-0003-0947-9479

Stefano Alcaro − *Dipartimento di Scienze della Salute, Università "Magna Græcia" di Catanzaro, Catanzaro 88100, Italy; Net4Science Academic Spin-Off, Università "Magna Græcia" di Catanzaro, Catanzaro 88100, Italy*; orcid.org/0000-0002-0437-358X

Complete contact information is available at: https://pubs.acs.org/10.1021/acsomega.4c06244

Author Contributions

The manuscript was written through contributions of all authors. All authors have given approval to the final version of the manuscript.

Notes

The authors declare no competing financial interest.

ACKNOWLEDGMENTS

Mass spectrometry analyses of aegPNA and NMR interaction studies were performed at the mass spectrometry and NMR facilities of Unitech COSPECT, University of Milano. The authors acknowledge the Italian Ministero dell'Università e della Ricerca (MUR) for the doctoral fellowship to I.G. and M.G. F.V. acknowledges PSR (Piano sostegno alla ricerca) 2023 from University of Milano. This research was funded by the Italian University Ministry Project "ONE HEALTH BASIC AND TRANSLATIONAL RESEARCH ACTIONS (INF-ACT)" grant number PE13_INFACT_PNRR-U.A. 14.01, CUP F13C22001220007 to S.C.

ABBREVIATIONS

3′-UTR, 3′-untranslated region
aegPNA, *N*-2-aminoethylglycine peptide nucleic acid
ARE, adenine−uridine-rich element
CF, cystic fibrosis
ELAV, embryonic lethal abnormal vision
FP, fluorescence polarization
MD, molecular dynamic
NMP, *N*-methyl pyrrolidone
RBPs, RNA-binding proteins
REMSAs, RNA-electrophoresis mobility shift assays
RMSD, root-mean-square deviation
RNases, ribonucleases
RRM, RNA-recognition motif
SMol, small molecule
STD-NMR, saturation transfer difference NMR

https://doi.org/10.1021/acsomega.4c06244
ACS Omega 2024, 9, 45147−45158

REFERENCES

(1) Hentze, M. W.; Castello, A.; Schwarzl, T.; Preiss, T. A Brave New World of RNA-Binding Proteins. *Nat. Rev. Mol. Cell Biol.* **2018**, *19* (5), 327−341.

(2) Udagawa, T.; Swanger, S. A.; Takeuchi, K.; Kim, J. H.; Nalavadi, V.; Shin, J.; Lorenz, L. J.; Zukin, R. S.; Bassell, G. J.; Richter, J. D. Bidirectional Control of mRNA Translation and Synaptic Plasticity by the Cytoplasmic Polyadenylation Complex. *Mol. Cell* **2012**, *47* (2), 253−266.

(3) Pascale, A.; Govoni, S. The Complex World of Post-Transcriptional Mechanisms: Is Their Deregulation a Common Link for Diseases? Focus on ELAV-like RNA-Binding Proteins. *Cell. Mol. Life Sci. CMLS* **2012**, *69* (4), 501−517.

(4) Jones, V. S.; Huang, R.-Y.; Chen, L.-P.; Chen, Z.-S.; Fu, L.; Huang, R.-P. Cytokines in Cancer Drug Resistance: Cues to New Therapeutic Strategies. *Biochim. Biophys. Acta* **2016**, *1865* (2), 255−265.

(5) Dong, R.; Yang, G.-D.; Luo, N.-A.; Qu, Y.-Q. HuR: A Promising Therapeutic Target for Angiogenesis. *Gland Surg.* **2014**, *3* (3), 203−206.

(6) Ye, X.; Fu, Q.; Xiao, H. The Role of RNA-Binding Protein HuR in Lung Cancer by RNA Sequencing Analysis. *Front. Genet.* **2022**, *13*, No. 813268.

(7) Wu, X.; Xu, L. The RNA-Binding Protein HuR in Human Cancer: A Friend or Foe? *Adv. Drug Delivery Rev.* **2022**, *184*, No. 114179.

(8) Badaoui, M.; Sobolewski, C.; Luscher, A.; Bacchetta, M.; Köhler, T.; van Delden, C.; Foti, M.; Chanson, M. Targeting HuR-Vav3 mRNA Interaction Prevents Pseudomonas Aeruginosa Adhesion to the Cystic Fibrosis Airway Epithelium. *JCI Insight* **2023**, *8* (3), No. e161961.

(9) Joseph, B. P.; Weber, V.; Knüpfer, L.; Giorgetti, A.; Alfonso-Prieto, M.; Krauß, S.; Carloni, P.; Rossetti, G. Low Molecular Weight Inhibitors Targeting the RNA-Binding Protein HuR. *Int. J. Mol. Sci.* **2023**, *24* (17), 13127.

(10) Mehta, M.; Raguraman, R.; Ramesh, R.; Munshi, A. RNA Binding Proteins (RBPs) and Their Role in DNA Damage and Radiation Response in Cancer. *Adv. Drug Delivery Rev.* **2022**, *191*, No. 114569.

(11) Sun, Y.; Zhan, S.; Zhao, S.; Zhong, T.; Wang, L.; Guo, J.; Dai, D.; Li, D.; Cao, J.; Li, L.; Zhang, H. HuR Promotes the Differentiation of Goat Skeletal Muscle Satellite Cells by Regulating Myomaker mRNA Stability. *Int. J. Mol. Sci.* **2023**, *24* (8), 6893.

(12) Raguraman, R.; Shanmugarama, S.; Mehta, M.; Peterson, J. E.; Zhao, Y. D.; Munshi, A.; Ramesh, R. Drug Delivery Approaches for HuR-Targeted Therapy for Lung Cancer. *Adv. Drug Delivery Rev.* **2022**, *180*, No. 114068.

(13) Vasile, F.; Della Volpe, S.; Ambrosio, F. A.; Costa, G.; Unver, M. Y.; Zucal, C.; Rossi, D.; Martino, E.; Provenzani, A.; Hirsch, A. K. H.; Alcaro, S.; Potenza, D.; Collina, S. Exploration of Ligand Binding Modes towards the Identification of Compounds Targeting HuR: A Combined STD-NMR and Molecular Modelling Approach. *Sci. Rep.* **2018**, *8* (1), 1−11.

(14) Volpe, S. D.; Listro, R.; Parafioriti, M.; Di Giacomo, M.; Rossi, D.; Ambrosio, F. A.; Costa, G.; Alcaro, S.; Ortuso, F.; Hirsch, A. K. H.; Vasile, F.; Collina, S. BOPC1 Enantiomers Preparation and HuR Interaction Study. From Molecular Modeling to a Curious DEEP-STD NMR Application. *ACS Med. Chem. Lett.* **2020**, *11* (5), 883−888.

(15) Meisner, N.-C.; Hintersteiner, M.; Mueller, K.; Bauer, R.; Seifert, J.-M.; Naegeli, H.-U.; Ottl, J.; Oberer, L.; Guenat, C.; Moss, S.; Harrer, N.; Woisetschlaeger, M.; Buehler, C.; Uhl, V.; Auer, M. Identification and Mechanistic Characterization of Low-Molecular-Weight Inhibitors for HuR. *Nat. Chem. Biol.* **2007**, *3* (8), 508−515.

(16) D'Agostino, V. G.; Adami, V.; Provenzani, A. A Novel High Throughput Biochemical Assay to Evaluate the HuR Protein-RNA Complex Formation. *PloS One* **2013**, *8* (8), No. e72426.

(17) D'Agostino, V. G.; Lal, P.; Mantelli, B.; Tiedje, C.; Zucal, C.; Thongon, N.; Gaestel, M.; Latorre, E.; Marinelli, L.; Seneci, P.; Amadio, M.; Provenzani, A. Dihydrotanshinone-I Interferes with the RNA-Binding Activity of HuR Affecting Its Post-Transcriptional Function. *Sci. Rep.* **2015**, *5*, 16478.

(18) Yu, J.; Lan, L.; Lewin, S. J.; Rogers, S. A.; Roy, A.; Wu, X.; Gao, P.; Karanicolas, J.; Aubé, J.; Sun, B.; Xu, L. Identification of Novel Small Molecule Beclin 1 Mimetics Activating Autophagy. *Oncotarget* **2017**, *8* (31), 51355−51369.

(19) Della Volpe, S.; Nasti, R.; Queirolo, M.; Unver, M. Y.; Jumde, V. K.; Dömling, A.; Vasile, F.; Potenza, D.; Ambrosio, F. A.; Costa, G.; Alcaro, S.; Zucal, C.; Provenzani, A.; Di Giacomo, M.; Rossi, D.; Hirsch, A. K. H.; Collina, S. Novel Compounds Targeting the RNA-Binding Protein HuR. Structure-Based Design, Synthesis, and Interaction Studies. *ACS Med. Chem. Lett.* **2019**, *10* (4), 615−620.

(20) Della Volpe, S.; Linciano, P.; Listro, R.; Tumminelli, E.; Amadio, M.; Bonomo, I.; Elgaher, W. A. M.; Adam, S.; Hirsch, A. K. H.; Boeckler, F. M.; Vasile, F.; Rossi, D.; Collina, S. Identification of N,N-Arylalkyl-Picolinamide Derivatives Targeting the RNA-Binding Protein HuR, by Combining Biophysical Fragment-Screening and Molecular Hybridization. *Bioorganic Chem.* **2021**, *116*, No. 105305.

(21) Volpe, S. D.; Listro, R.; Ambrosio, F. A.; Garbagnoli, M.; Linciano, P.; Rossi, D.; Costa, G.; Alcaro, S.; Vasile, F.; Hirsch, A. K. H.; Collina, S. Identification of HuR-RNA Interfering Compounds by Dynamic Combinatorial Chemistry and Fluorescence Polarization. *ACS Med. Chem. Lett.* **2023**, *14* (11), 1509−1516.

(22) Garbagnoli, M.; Linciano, P.; Listro, R.; Rossino, G.; Vasile, F.; Collina, S. Biophysical Assays for Investigating Modulators of Macromolecular Complexes: An Overview. *ACS Omega* **2024**, *9* (16), 17691−17705.

(23) Yasgar, A.; Jadhav, A.; Simeonov, A.; Coussens, N. P. AlphaScreen-Based Assays: Ultra-High-Throughput Screening for Small-Molecule Inhibitors of Challenging Enzymes and Protein-Protein Interactions. *Methods Mol. Biol. Clifton NJ.* **2016**, *1439*, 77−98.

(24) Manzoni, L.; Zucal, C.; Maio, D. D.; D'Agostino, V. G.; Thongon, N.; Bonomo, I.; Lal, P.; Miceli, M.; Baj, V.; Brambilla, M.; Cerofolini, L.; Elezgarai, S.; Biasini, E.; Luchinat, C.; Novellino, E.; Fragai, M.; Marinelli, L.; Provenzani, A.; Seneci, P. Interfering with HuR-RNA Interaction: Design, Synthesis and Biological Characterization of Tanshinone Mimics as Novel, Effective HuR Inhibitors. *J. Med. Chem.* **2018**, *61* (4), 1483−1498.

(25) Chheda, U.; Pradeepan, S.; Esposito, E.; Strezsak, S.; Fernandez-Delgado, O.; Kranz, J. Factors Affecting Stability of RNA - Temperature, Length, Concentration, pH, and Buffering Species. *J. Pharm. Sci.* **2024**, *113* (2), 377−385.

(26) Suparpprom, C.; Vilaivan, T. Perspectives on Conformationally Constrained Peptide Nucleic Acid (PNA): Insights into the Structural Design, Properties and Applications. *RSC Chem. Biol.* **2022**, *3* (6), 648−697.

(27) Duffy, K.; Arangundy-Franklin, S.; Holliger, P. Modified Nucleic Acids: Replication, Evolution, and next-Generation Therapeutics. *BMC Biol.* **2020**, *18* (1), 112.

(28) Brennan, C. M.; Steitz, J. A. HuR and mRNA Stability. *Cell. Mol. Life Sci.* **2001**, *58* (2), 266−277.

(29) Doller, A.; Pfeilschifter, J.; Eberhardt, W. Signalling Pathways Regulating Nucleo-Cytoplasmic Shuttling of the mRNA-Binding Protein HuR. *Cell. Signal.* **2008**, *20* (12), 2165−2173.

(30) Wang, H.; Zeng, F.; Liu, Q.; Liu, H.; Liu, Z.; Niu, L.; Teng, M.; Li, X. The Structure of the ARE-Binding Domains of Hu Antigen R (HuR) Undergoes Conformational Changes during RNA Binding. *Acta Crystallogr. D Biol. Crystallogr.* **2013**, *69* (3), 373−380.

(31) Luppi, E.; Coccia, E. Probing the Molecular Frame of Uracil and Thymine with High-Harmonic Generation Spectroscopy. *Phys. Chem. Chem. Phys. PCCP* **2021**, *23* (6), 3729−3738.

(32) Vértessy, B. G.; Tóth, J. Keeping Uracil out of DNA: Physiological Role, Structure and Catalytic Mechanism of dUTPases. *Acc. Chem. Res.* **2009**, *42* (1), 97−106.

(33) Boncel, S.; Gondela, A.; Walczak, K. Uracil as a Target for Nucleophilic and Electrophilic Reagents. *Curr. Org. Synth.* **2008**, *5* (4), 365−396.

https://doi.org/10.1021/acsomega.4c06244
ACS Omega 2024, 9, 45147−45158

(34) Nielsen, P. E. *Peptide Nucleic Acids: Protocols and Applications*; Horizon Scientific Press: Wymondham, Norfolk, U.K., 2004, 2nd Ed.
(35) Ferrige, A.; Seddon, M. J.; Jarvis, S.; Skilling, J.; Aplin, R. Maximum Entropy Deconvolution in Electrospray Mass Spectrometry. *Rapid Commun. Mass Spectrom.* **1991**, *5*, 374.
(36) *Schrödinger Release 2019−3: Protein Preparation Wizard*; Schrödinger, LLC: New York, N.Y., 2019.
(37) *Protein Preparation Wizard*; Schrödinger, LLC: New York, N.Y., 2018−1.
(38) *Protein Preparation Wizard*; Schrödinger LLC: New York, NY, 2018.
(39) *Schrödinger Release 2018−1: Maestro*; Schrödinger LLC: New York, NY, 2018.
(40) *Desmond Molecular Dynamics System*, D.E. Shaw Research: New York, NY, 2018.
(41) *Desmond Molecular Dynamics System, D.E. Shaw Research. New York, NY, 2018; Maestro-Desmond Interoperability Tools*; Schrödinger: New York, NY, 2018.
(42) *ADMETlab 2.0*. https://admetmesh.scbdd.com/.
(43) Xiong, G.; Wu, Z.; Yi, J.; Fu, L.; Yang, Z.; Hsieh, C.; Yin, M.; Zeng, X.; Wu, C.; Lu, A.; Chen, X.; Hou, T.; Cao, D. ADMETlab 2.0: An Integrated Online Platform for Accurate and Comprehensive Predictions of ADMET Properties. *Nucleic Acids Res.* **2021**, *49* (W1), W5−W14.

https://doi.org/10.1021/acsomega.4c06244
ACS Omega 2024, 9, 45147−45158